Cell, Vol. 118, 767–780, September 17, 2004, Copyright ©2004 by Cell Press

Caveolin-Stabilized Membrane Domains as Multifunctional Transport and Sorting Devices in Endocytic Membrane Traffic

Lucas Pelkmans,[1,*] Thomas Bürli,[2] Marino Zerial,[1] and Ari Helenius[2]
[1]Max Planck Institute for Molecular Cell Biology and Genetics
01307 Dresden
Germany
[2]Institute of Biochemistry
Swiss Federal Institute of Technology
CH-8093 Zurich
Switzerland

Summary

Endocytosis comprises several routes of internalization. An outstanding question is whether the caveolar and endosomal pathways intersect. Following transport of the caveolar protein Caveolin-1 and two cargo complexes, Simian Virus 40 and Cholera toxin, in live cells, we uncovered a Rab5-dependent pathway in which caveolar vesicles are targeted to early endosomes and form distinct and stable membrane domains. In endosomes, the low pH selectively allowed the toxin to diffuse out of the caveolar domains into the surrounding membrane, while the virus remained trapped. Thus, we conclude that, unlike cyclic assembly and disassembly of coat proteins in vesicular transport, oligomeric complexes of caveolin-1 confer permanent structural stability to caveolar vesicles that transiently interact with endosomes to form subdomains and release cargo selectively by compartment-specific cues.

Introduction

Endocytosis in animal cells involves multiple mechanisms that differ in type of cargo, in mode of vesicle formation, and in intracellular fate of internalized cargo (Conner and Schmid, 2003; Gruenberg, 2001; Mellman, 1996). The mechanisms include phagocytosis, macropinocytosis, clathrin-dependent endocytosis, and clathrin-independent uptake mechanisms such as caveolae-mediated endocytosis, which internalize ligands and molecules associated with lipid rafts in the plasma membrane (Parton and Richards, 2003).

The composition and morphology of early endosomes, which most incoming ligands encounter as the first sorting compartment, reflects the broad functional diversity of endocytic organelles. A mosaic of distinct domains in the limiting endosomal membrane regulates in- and outgoing vesicle traffic (Gruenberg, 2001; Zerial and McBride, 2001). The small GTPase Rab5 serves as one of the central organizers. It orchestrates the assembly of multimeric effector complexes on the early endosome membrane needed to regulate fusion of incoming vesicles, to support homotypic fusion between early endosomes, and to mediate transport along microtubules. Other Rab GTPases of early and recycling endosomes are segregated into distinct membrane domains that display different biochemical composition and pharmacological properties (Gruenberg, 2001; Zerial and McBride, 2001).

Less extensively documented is the trafficking of caveolae to a recently described endocytic organelle, the caveosome. Caveolae are lipid raft-enriched, flask-shaped, Caveolin-1-containing invaginations present in the plasma membrane of many cell types (Anderson, 1998), and caveosomes are intracellular Caveolin-1-containing membrane-bounded structures of neutral pH, distinct from classical endocytic compartments (Pelkmans et al., 2001). The most abundant structural components of the caveolar membrane are oligomers of Caveolin-1, a cholesterol binding integral membrane protein essential for the formation of caveolae (Drab et al., 2001; Fra et al., 1995; Monier et al., 1995; Murata et al., 1995; Rothberg et al., 1992). Caveolin-1 oligomers form filamentous structures that are believed to stabilize the membrane and to define the size and shape of caveolae (Fernandez et al., 2002). These are fixed in the plasma membrane of living cells and do not exchange Caveolin-1 molecules by lateral diffusion (Thomsen et al., 2002). Association of cargo with caveolar domains at the cell surface may involve interaction with Caveolin-1 itself or with components of the lipid raft-enriched membrane in the caveolae (Parton and Richards, 2003).

Simian virus 40 (SV40) (Anderson et al., 1996; Stang et al., 1997) and Cholera toxin (ChTx) (Orlandi and Fishman, 1998; Parton et al., 1994) are the best-studied caveolar ligands. Both bind to a ganglioside (GM1) (Heyningen, 1974; Tsai et al., 2003) and are transported by caveolar endocytosis to caveosomes (Nichols, 2002; Pelkmans et al., 2001). SV40 is sorted from caveosomes into vesicular and tubular membrane structures that travel along microtubules to the smooth ER (Pelkmans et al., 2001). Only transiently are some SV40 particles seen in endosomes early after internalization (Kartenbeck et al., 1989). In contrast, ChTx passes through early endosomes and accumulates in the Golgi complex (Richards et al., 2002; Tran et al., 1987). SV40 and ChTx can thus take different trafficking routes after internalization.

The existence of two caveolar trafficking routes involving caveosomes and early endosomes raises a number of questions concerning their interdependence. Do incoming caveolae or the downstream caveosomes interact with the classical endocytic compartments or with compartments of the secretory pathway? How does molecular sorting of cargo take place, and how is the trafficking and recycling of structural components of caveolae regulated? On the plasma membrane, caveolae are thought to be stable structures. However, do the structural components of caveolae disassemble in the course of trafficking to release cargo upon fusion of the vesicles with the organelle membrane? By analyzing the involvement of several small GTPases in the trafficking of caveolae and the cargo in live cells, and by determining the lateral mobility of Caveolin-1, SV40, ChTx, and other components in endocytic membranes, we found that

*Correspondence: pelkmans@mpi-cbg.de

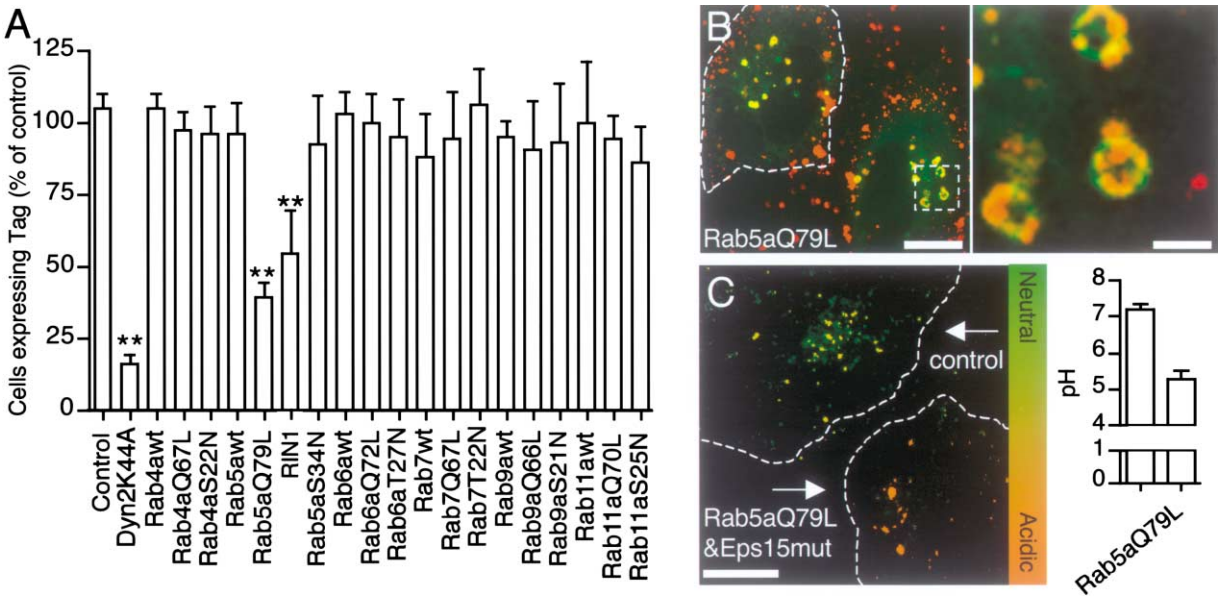

Figure 1. Effects of RabGTPases on SV40 Infection and Trafficking

(A) HeLa cells expressing indicated Rab constructs or RIN1 were infected with SV40 at a multiplicity of infection (MOI) of 5. After infection (16 hr), cells were fixed and immunostained for large T antigen (Tag). The fraction of Tag-expressing cells of at least 120 transfected cells from three different experiments was determined and presented as percentage of nontransfected control cells. Dynamin2K44A (Dyn2K44A) was used as a positive control. Of the Rab constructs, only expression of Rab5aQ79L interfered with SV40 infection. Asterisks indicate significant Student's t test values ($p < 0.001$).

(B) In cells expressing GFP-Rab5Q79L, AF647-SV40 internalized for 2 hr accumulates in enlarged endosomes. The cell indicated with a white line additionally expresses a truncation mutant of Eps15, which blocks clathrin-coated pit assembly, showing that transport of SV40 to the enlarged endosomes was independent of clathrin-mediated uptake. Scale bars, 10 μm and 2.5 μm.

(C) Two cells, one nontransfected (control) and one coexpressing Rab5Q79L and a mutant of Eps15 (detected by its RFP tag), incubated with FLX-SV40 for 2 hr were analyzed live with confocal microscopy to measure the pH in which the virus particles reside. The 520 nm emission was measured by excitation at two different wavelengths (440 nm and 488 nm) and the ratio between the two images calculated and pseudocolored. A calibration curve to calculate the pH was obtained from ionophore-treated cells in media of different pH (Pelkmans et al., 2001). Green color indicates a neutral compartment, while orange color indicates an acidic compartment. In the cell expressing Rab5Q79L, most SV40 resides in an acidic compartment of pH 5.3. Scale bar, 10 μm.

caveolae function by mechanisms quite different from other transport vesicles.

Results

Effects of RabGTPases on SV40 Entry and Infection

Since RabGTPases are known to play distinct, regulatory roles in membrane transport, we tested whether any of those known to be associated with endosome and Golgi function would serve as regulators of caveolae-mediated endocytosis. To test their functional involvement, we overexpressed wild-type, constitutively active (GTP binding), and inactive (GDP binding) forms of the Rab proteins and determined whether they interfered with SV40 infection. Remarkably, the dominant-active mutant of Rab5 (Rab5aQ79L) was the only mutant among the Rab proteins tested that inhibited SV40 infection. Consistently, overexpression of RIN1, a Rab5 GEF (Tall et al., 2001), also reduced SV40 infection. None of the other wild-type or mutant Rab proteins inhibited SV40 infection (Figure 1A), suggesting that they are not required for SV40 internalization, transport to caveosomes, and subsequent transport to the smooth endoplasmic reticulum (sER).

Consistently, incoming Alexa Fluor-labeled SV40 particles failed to show significant colocalization with green fluorescent protein (GFP)-tagged wild-type Rab4a, Rab6a, Rab7, Rab9a, and Rab11a in live CV-1 cells or HeLa cells (see Supplemental Figure S1A at http://www.cell.com/cgi/content/full/118/6/767/DC1). A small although significant fraction of SV40 (20% ± 6%) did, however, colocalize with GFP-Rab5a, in agreement with our previous electron microscopy studies showing some viruses in structures resembling early endosomes (Kartenbeck et al., 1989). The effect of activated Rab5 on SV40 infection together with the localization data prompted us to further investigate the role of Rab5a in caveolar endocytosis.

Rab5aQ79L Causes SV40 Rerouting

The Rab5aQ79L mutant generates abnormally enlarged endosomes by stimulating homotypic fusion of early endosomes (Stenmark et al., 1994). In cells expressing GFP-Rab5aQ79L, we observed that incoming Alexa Fluor-labeled SV40 particles were not transported to caveosomes as in control cells but were trapped into Rab5aQ79L-GFP-positive endosomes (Figure 1B). The Rab5S34N mutant did not influence SV40 internalization or trafficking (data not shown).

In the enlarged endosomes, the fluorescent SV40 particles were not distributed uniformly but formed patches along the limiting membrane (Figure 1B). When fluores-

cein-labeled SV40 particles were internalized into such endosomes, the pH of their environment could be estimated by exciting the fluorophore at 488 and 454 nm. SV40 particles in enlarged endosomes were exposed to pH 5.3 ± 0.4, while SV40 particles in control cells were exposed to pH 7.2 ± 0.3 (Figure 1C) (Pelkmans et al., 2001). Apparently, the SV40-carrying vesicles had actually fused with the membrane of the acidic enlarged endosomes.

Coexpression of Rab5aQ79L and a mutant of Eps15 (Eps15EΔ95/295) that effectively blocks clathrin-coated pit assembly (Benmerah et al., 1999) did not block SV40 internalization into endosomes, while it reduced Alexa Fluor-labeled transferrin internalization to 70% (Figure 1C and Supplemental Figure S1B on the *Cell* web site). SV40 was therefore unlikely to be transported to the endosomes by clathrin-mediated uptake despite the stimulation by constitutively active Rab5a (Stenmark et al., 1994). However, transport of SV40 in the enlarged endosomes was blocked by expression of Dyn2K44A, by cholesterol depletion, and by inhibition of tyrosine kinases (data not shown), treatments known to block caveolar uptake of SV40 (Pelkmans et al., 2002). We conclude that expression of constitutively active Rab5 resulted in intracellular retargeting of virus particles endocytosed through caveolae to early endosomes. This diversion from the normal itinerary to caveosomes apparently interfered with SV40 infection, consistent with our previous observation that SV40 has to reach the ER to be infectious (Pelkmans et al., 2001).

Caveolin-1 in Early Endosomes

To analyze the pathways taken by SV40 in further detail, we established a HeLa cell line stably expressing Caveolin-1 with GFP fused to its C terminus (Cav1-GFP) at levels similar to the endogenous protein (Supplemental Figure S1C). We have shown previously that, when expressed transiently in these amounts, the GFP-tagged protein behaves like the endogenous protein and supports SV40 entry (Pelkmans et al., 2001). Using 3D deconvolution of optical stacks from 34 cells (Experimental Procedures and Supplemental Figure S1C), we determined that, at steady state, 12% ± 4% colocalized with the Golgi complex marker giantin, and 15% ± 6% colocalized with EEA1-positive early endosomes. To detect EEA1-negative early endosomes, we internalized fluorescent transferrin for 2 min and found that 18% ± 7% of Cav1-GFP colocalized with it (Supplemental Figure S1D). Of the remaining 70% ± 10%, the majority was present in caveolae on the cell surface and in intracellular structures, presumably caveosomes.

To explore the distribution of Cav1-GFP within early endosomes, we made surface-rendered, 3D reconstructions of the deconvolved stacks (Figures 2A and 2B). The Cav1-GFP signal appeared as small vesicles and as larger structures with irregular shape. The latter seemed composed of clusters of small vesicles, consistent with electron microscopy images of caveosomes (Pelkmans et al., 2001; Peters et al., 2003). On early endosomes, Cav1-GFP appeared as partially protruding structures with a similar, sometimes clustered morphology. These had a limited overlap with or excluded EEA1 (Figure 2B) and were not stained by a double FYVE construct (2XFYVE) (Campbell et al., 2002) tagged with monomeric red fluorescent protein (Gillooly et al., 2000), indicating that the caveolar domains did not incorporate the early endosome-enriched lipid phosphatidyl inositol 3-phosphate (PI[3]P) (Supplemental Figures S2A and S2B). The Cav1-GFP-labeled patches thus represented distinct domains in the mosaic of subdomains characterizing the limiting membrane of early endosomes. Likely, these domains correspond to the caveolin-1-positive subdomains on endosomes visualized recently with immunoelectron microscopy (Peters et al., 2003).

Time-lapse confocal imaging of cells coexpressing Cav1-GFP and mRFP-Rab5a revealed that interactions between Cav1-GFP-positive and mRFP-Rab5a-positive structures were frequent but transient. Small Cav1-GFP-labeled vesicles were seen to bind to larger Rab5a-positive structures, to move along with them for up to 20 s as part of a complex, and then to detach (Figure 2C and Supplemental Movie S1). We could also see similar vesicles interacting with larger Cav1-GFP-positive caveosomes, suggesting dynamic interactions with these organelles as well.

Rab5 Targets Caveolar Vesicles to Early Endosomes

To test whether the transient interactions of caveolar vesicles with early endosomes were dependent on Rab5, we examined the effects of perturbations of the Rab5 nucleotide cycle on the colocalization of Cav1-GFP with EEA1. In cells expressing low levels of constitutively inactive Rab5 (Rab5S34N) that still had vesicles stained for EEA1, the overlap of Cav1-GFP with EEA1 was substantially diminished (Figure 2D and Supplemental Figure S2C). In contrast, in cells expressing Rab5Q79L, most of the intracellular Cav1-GFP was localized in the enlarged endosomes (Figure 2D and Supplemental Figures S2D and S2E). In these cells, Cav1-GFP-labeled caveosomes were strongly reduced but not completely absent, judging by the presence of some larger Cav1-GFP-positive but Rab5Q79L- and EEA1-negative structures (arrowhead, Supplemental Figure S2D). When fluorescent SV40 particles were added to Rab5Q79L- and Cav1-GFP-expressing cells, they were internalized and localized to the Cav1-GFP-positive patches (Figure 2E). Because the viruses were exposed to the acidic lumen (see Figure 1C), the Cav1-GFP-positive patches were in membrane continuity with the enlarged endosomes.

3D surface reconstructions suggested that, in the presence of active Rab5, the small Cav1-GFP-positive vesicles in the cytosol were lost and were now distributed over the membrane of the enlarged endosomes (Figure 2F). However, a maximum intensity projection of a deconvolved stack of two enlarged endosomes containing fewer Cav1-GFP patches revealed that the membrane compartmentalization of Cav1-GFP was retained within the early endosomes (Figure 2G). Time-lapse imaging revealed that caveolar domains were trapped on the enlarged endosomes (Figure 2H and Supplemental Movie S2).

Consistently, we found that overexpression of RN-tre, a Rab5 GAP (Lanzetti et al., 2000), completely abolished the overlap of endogenous Caveolin-1 with EEA1 (Figure

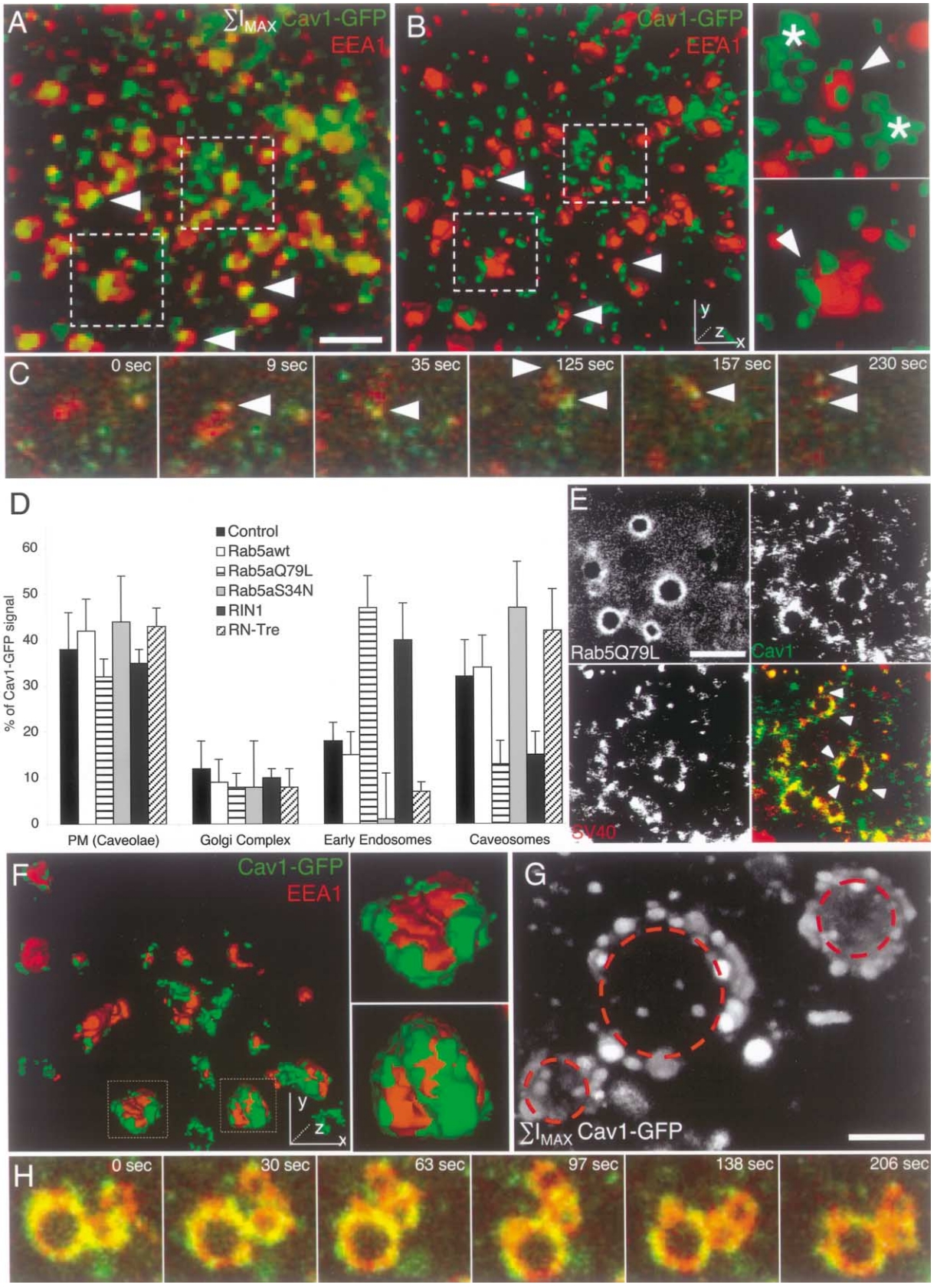

Figure 2. Caveolar Subdomains on Endosomes Trapped by Rab5Q79L

(A) HeLa cells stably expressing Cav1-GFP were fixed and immunostained against EEA1 to label early endosomes. The maximum intensity projection of a Z stack of 40 deconvolved sections is depicted. Scale bar, 3 μm.

2D and Supplemental Figure S3A). Conversely, overexpression of RIN1, a Rab5 GEF (Tall et al., 2001), increased the presence of endogenous Caveolin-1 on early endosomes (Figure 2D and Supplemental Figure S3B). The latter results argued that endogenous Rab5 regulates the interaction of caveolar domains with early endosomes.

In summary, the results indicate that caveolar vesicles can move from caveosomes to early endosomes in a Rab5a-dependent process. Although they dock and fuse with the endosomal membrane, they form subdomains that do not intermix with the surrounding membrane. After some time, the caveolin-1 patches pinch off again as membrane vesicles. Perturbation of this cycle by expression of Rab5aQ79L results in accumulation of caveolar domains on endosomes at the expense of caveosomes and trapping of SV40. Likely, under normal conditions, caveolar vesicles carrying SV40 particles also transiently interact with early endosomes. For SV40 infection, however, this is not obligatory, because constitutively inactive Rab5 does not inhibit SV40 infectious entry (Figure 1).

Rab5 Regulates Traffic between Early Endosomes and Caveosomes

Since internalized ChTx has been observed in compartments of the classical endosomal system as well as in caveosomes (Nichols, 2002; Richards et al., 2002; Sandvig and van Deurs, 2002), we wondered whether it might utilize the Rab5-dependent pathway from caveolae to endosomes. To address this question, we needed to follow ChTx internalized specifically via caveolae and not via other pathways by which it can reach early endosomes (Parton and Richards, 2003). We noticed that, when added in very low amounts (100 pg, ~50,000 molecules/cell), virtually all Alexa Fluor-labeled ChTx B subunits (AF-ChTxB) accumulated in Cav1-GFP-positive structures 10 min after addition and were not observed in early endosomes (Figure 3A). This suggested that, at low concentrations, the toxin was entering predominantly by the caveolar pathway.

Over time, we observed ChTxB colocalizing with EEA1 and accumulating in the Golgi complex. Expression of constitutively inactive Rab5a strongly reduced colocalization with EEA1 and blocked accumulation of the toxin in the Golgi complex at later time points (Figures 3B and 3C). However, it did not significantly block internalization of the toxin (Supplemental Figure S4A). In cells expressing constitutively active Rab5a, colocalization of ChTxB with EEA1 in enlarged endosomes was increased, and transport to the Golgi complex took place (Figure 3C). Accumulation in the enlarged endosomes was not reduced by coexpressing mutant Eps15, indicating that the toxin was not internalized into enlarged endosomes by clathrin-coated pits (Supplemental Figure S4B).

In summary, the results indicated that, in HeLa cells stably expressing Cav1-GFP, ChTxB is transported to endosomes by caveolar vesicles in a process dependent on Rab5. If intracellular caveolar vesicles transiently fuse with early endosomes, they should be able to pick up some fluid phase from that compartment and potentially ferry it to caveosomes. To test this, we incubated cells in high amounts of the fluid phase tracer Lucifer yellow (LY) for a long time (90 min) and observed that a small but significant fraction (~30%) of LY accumulates in caveolar vesicles and caveosomes, either in the presence or absence of a caveolar ligand (Supplemental Figures S4C and S4D). Because cell surface caveolae do not travel to intracellular caveosomes in the absence of a stimulus (Thomsen et al., 2002), LY is likely to arrive there by another route, presumably via early endosomes. In agreement, we observed that, in cells expressing Rab5aS34N, LY accumulation in caveolar vesicles or caveosomes is completely blocked, while overall fluid phase uptake is only slightly reduced (Supplemental Figure S4D). Apparently, not only do caveolar vesicles ferry ChTxB to early endosomes, they also ferry some fluid phase from early endosomes to caveosomes, which suggests that traffic is bidirectional.

Caveolar Domains in Endosomes Serve as Stable Scaffolds

During confocal analysis of Rab5Q79L-enlarged endosomes, we observed that, while SV40 particles remained continuously localized in the Caveolin-1 patches, ChTxB showed this restricted distribution only occasionally and only at early time points after internalization. In most cases, the toxin was found more evenly distributed in the membrane of the endosomes. To study the lateral diffusion of these ligands and of endogenous endosome molecules, we used fluorescence recovery after photobleaching (FRAP) on individual Rab5Q79L-enlarged en-

(B) Surface-rendered 3D reconstructions were made of each channel (green, Cav1-GFP; red, EEA1). Enlargements on the right show caveosomes (asterisks) and caveolar domains on early endosomes. 3D scale bar, 2.5 μm.

(C) Images of a time-lapse sequence (Supplemental Movie S1) displaying the mobility of Cav1-GFP-positive vesicles (green) and their transient interaction (arrowheads) with Rab5wt-RFP-positive structures (red).

(D) Quantification of deconvolved optical stacks of Cav1-GFP-expressing cells stained for EEA1 (see Supplemental Figures S2 and S3): Rab5aQ79L recruits predominantly intracellular but not Golgi complex-derived Cav1-GFP to early endosomes. Rab5aS34N expression results in a strong reduction of Cav1-GFP on early endosomes. Expression of the Rab5GEF RIN1 has similar effects as Rab5aQ79L, while expression of the Rab5GAP RN-tre shows similar effects as Rab5aS34N. Overexpression of Rab5awt does not affect Cav1-GFP distribution compared to nontransfected (control) cells.

(E) Confocal analysis of internalized SV40 into enlarged endosomes reveals that the spot-like pattern colocalizes with Caveolin-1 spots on the endosome membrane. Scale bar, 3 μm.

(F) Surface-rendered, 3D reconstruction of an optical stack from a Rab5Q79L-expressing cell (area depicted in Supplemental Figure S2C) of the Cav1-GFP and EEA1 signals. Cav1-GFP patches cover large parts of the enlarged endosomes. 3D scale bar, 1.5 μm.

(G) A maximum intensity projection of a Z stack containing the deconvolved signal of Cav1-GFP on three enlarged endosomes (indicated by dashed circles). Scale bar, 1 μm.

(H) Images of a time-lapse sequence (Supplemental Movie S1) displaying entrapped Cav1-GFP-positive domains (green) on Rab5Q79L-RFP-positive structures (red).

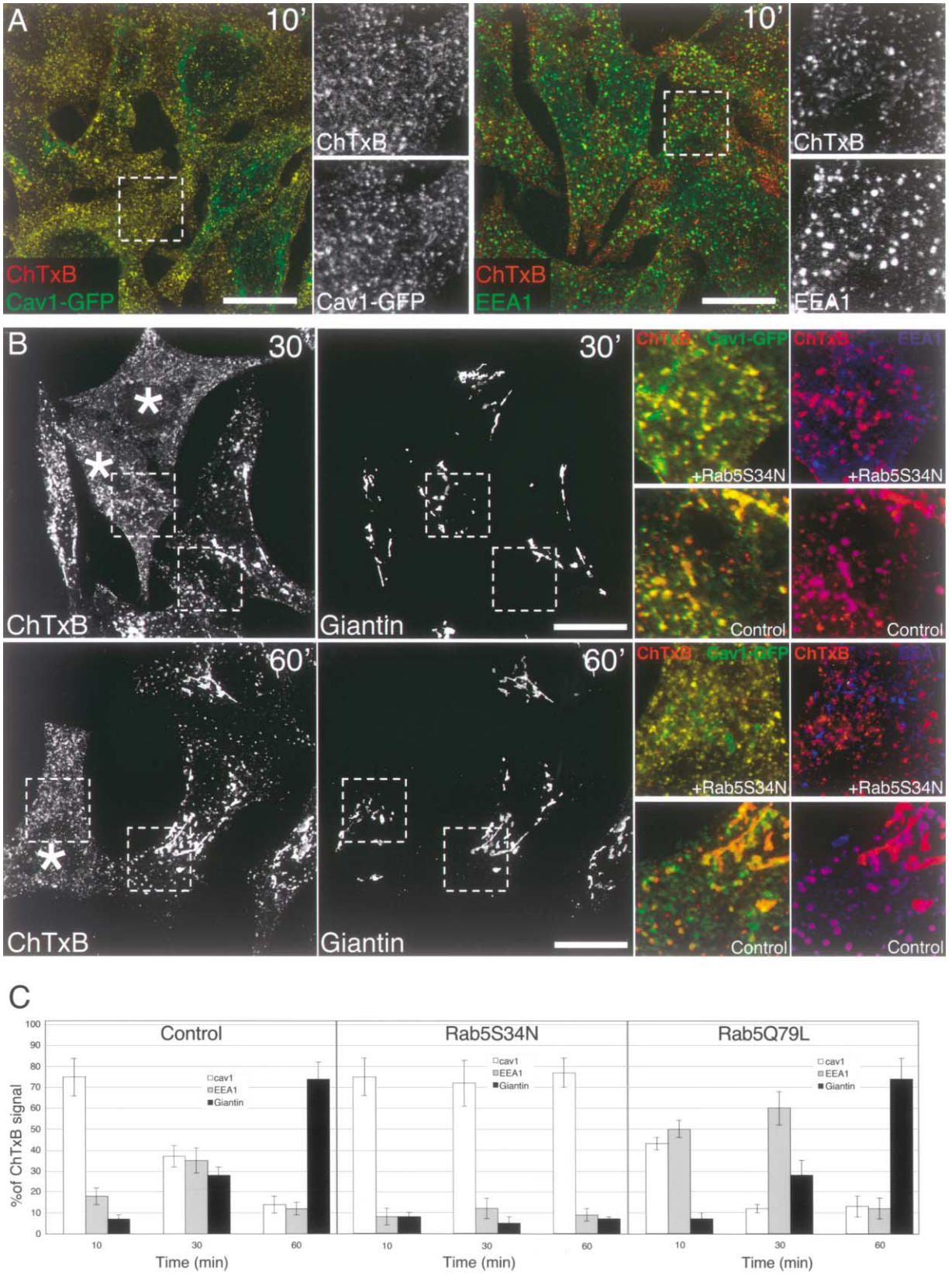

Figure 3. Rab5 Directs ChTx to Endosomes, Which Is Necessary to Accumulate in the Golgi Complex

(A) Cav1-GFP-expressing HeLa cells were incubated with 100 pg of AF-ChTxB for 10 min. All AF-ChTxB colocalizes with Cav1-GFP at this time point (left) and not with EEA1 (right). Scale bars, 20 μm.

(B) Cav1-GFP-expressing HeLa cells were transiently transfected with Rab5aS34N (transfected cells indicated with asterisks). In cells expressing

dosomes that contained Cav1-GFP domains. Although enlarged endosomes are aberrant structures, they had advantages for FRAP experiments: they are bigger and more stationary than normal endosomes, they show little lateral and rotational mobility, and they have easily distinguished membrane domains.

To determine the dynamics of cellular molecules continuously or transiently resident in endosomes, we analyzed GFP-Rab5Q79L, GFP-tagged mannose-6-phosphate receptor (GFP-M6PR), GFP-tagged clathrin light chain (GFP-CLC), and Alexa Fluor-labeled transferrin (AF-Tfn). In addition, we analyzed glycosyl phosphatidyl inositol-anchored GFP (GPI-GFP), a lipid raft marker (Keller et al., 2001); BODIPY-labeled lactosyl ceramide (LacCer), a lipid probe that is thought to localize to caveolar membranes (Puri et al., 2001); and 2XFYVE-GFP that binds PI(3)P, an endosomal-enriched lipid (Gillooly et al., 2000). After quantification of the fluorescence signal of the bleached and unbleached parts of the endosomes (examples are depicted in Figure 4A), the recovery curves, corrected for bleaching caused by imaging, were fitted to a 2D diffusion model (see Experimental Procedures) and kinetic parameters determined (Figure 4B and Table 1). To correct for the fraction of recovery that occurred by exchange of fluorescence between a cytosolic and a membrane bound pool, the curves obtained for GFP-Rab5Q79L, GFP-CLC, and 2XFYVE-GFP were compared with corresponding recovery curves recorded from fully bleached endosomes.

Using this approach, we were able to establish that Cav1-GFP and Alexa Fluor-labeled SV40 were virtually immobile in the membrane (Figure 4B and Table 1). Although endosomal GFP-CLC exchanges with a cytosolic pool, we considered it to be immobile in the membrane as well, since the recovery curve for a bleached subdomain could be completely attributed to exchange with new molecules from the cytosol (Figure 4B and Table 1). GFP-M6PR and GFP-Rab5Q79L displayed a restricted mobility in the endosomal membrane (Figure 4B and Table 1). For M6PR, this presumably reflects its incorporation into complexes cycling between the trans-Golgi network and endosomes (Pfeffer, 2003). The restricted mobility of Rab5 in the GTP bound form is also consistent with the existence of oligomeric effector complexes on the early endosome membrane (McBride et al., 1999). In contrast, AF-Tfn, BODIPY-LacCer, GPI-GFP, 2XFYVE-GFP, and AF-ChTxB were molecules that showed a more or less unrestricted mobility (Figure 4B and Table 1). Control experiments using Cav1 tagged with monomeric red fluorescent protein (mRFP) or GPI-anchored mRFP did not reveal kinetics different from the GFP-tagged molecules, indicating that the weak oligomerization property of GFP did not influence our measurements (data not shown). We concluded that Caveolin-1 was present in uniquely stable domains that seemed to serve as scaffolds preventing lateral movement of SV40 but not of ChTxB or lipid raft probes like GPI-GFP or BODIPY-LacCer.

To test more directly whether Caveolin-1 was responsible for the slow diffusion of SV40, we reduced the Caveolin-1 levels in HeLa cells by RNA interference. It was previously shown that internalization of ChTxB is not blocked when Caveolin-1 is depleted (Nichols, 2002). When the cells were treated with short interfering RNA (siRNA) against Caveolin-1, the level of Caveolin-1 was reduced by more than 90%, judged by both Western blot analysis (Figure 4C) and immunofluorescence (data not shown). SV40 still enters Caveolin-1-depleted HeLa cells, but infection is 30%–40% less efficient (Figure 4C).

In the enlarged endosomes of Caveolin-1-depleted cells expressing Rab5aQ79L, we found that SV40 particles remained attached to the limiting membrane, but now the FRAP recovery rates were much faster, i.e., comparable to those of the lipid raft markers ChTxB and GPI-GFP and the lipid probe BODIPY-LacCer (Figure 4E and Table 1). Interestingly, in these cells, SV40 infection was completely (95%–100%) inhibited. Expression of Rab5S34N in Caveolin-1-depleted cells did not lead to a further block in infection (Figure 4E). Altogether, these results suggest that Caveolin-1 restricts the lateral mobility of GM1 bound cargo by forming structured subdomains in the endosomal membrane. These prevent diffusion of SV40 particles into membranes of the classical endocytic system and thereby increase the efficiency to reach the endoplasmic reticulum and infect the cell.

Low pH Induces Release of ChTxB from Caveolar Domains

The difference in the distribution and mobility of fluorescently labeled ChTxB and SV40 in the enlarged endosomes was puzzling, considering that they use the same receptors and were, under our conditions, both internalized by caveolae. One major difference between both ligands is, however, that, in cell types expressing Caveolin-1, ChTx depends on exposure to low pH for intoxication (Janicot et al., 1991), while SV40 does not depend on acidic pH for infection (Upcroft, 1987). In an artificial liposome system, ChTxB has been shown to undergo a conformational change upon treatment with low pH that changes the membrane partitioning properties of the GM1 molecules to which the toxin is bound (McCann et al., 1997). To determine whether this could explain ChTxB's more homogeneous distribution and higher mobility in endosomes compared to SV40, we incubated cells with the weak base NH_4Cl, which neutralizes the

Rab5aS34N, AF-ChTxB does not accumulate in the giantin-stained Golgi complex at 30 or 60 min. Enlargements on the right show that, in Rab5aS34N-expressing cells, AF-ChTxB remains in Cav1-GFP-positive structures, while, in control cells, AF-ChTxB exits Cav1-GFP-positive structures and passes through EEA1-positive structures to the Golgi complex. Scale bar, 20 μm.

(C) Quantification of deconvolved optical stacks obtained from stable Cav1-GFP-expressing cells transfected with Rab5aS34N, Rab5aQ79L, or no additional construct at different time points after AF-ChTxB binding. Initially, most AF-ChTxB colocalizes with Cav1-GFP (10 min), which rapidly moves through EEA1-positive endosomes and accumulates in a giantin-positive Golgi complex at 60 min. In cells overexpressing Rab5aS34N (middle graph), ChTxB does not accumulate in the Golgi complex but remains colocalized with Cav1-GFP. In Rab5aQ79L-expressing cells, AF-ChTxB appears more rapidly and prominently in enlarged endosomes. Accumulation in the Golgi complex, however, is not affected.

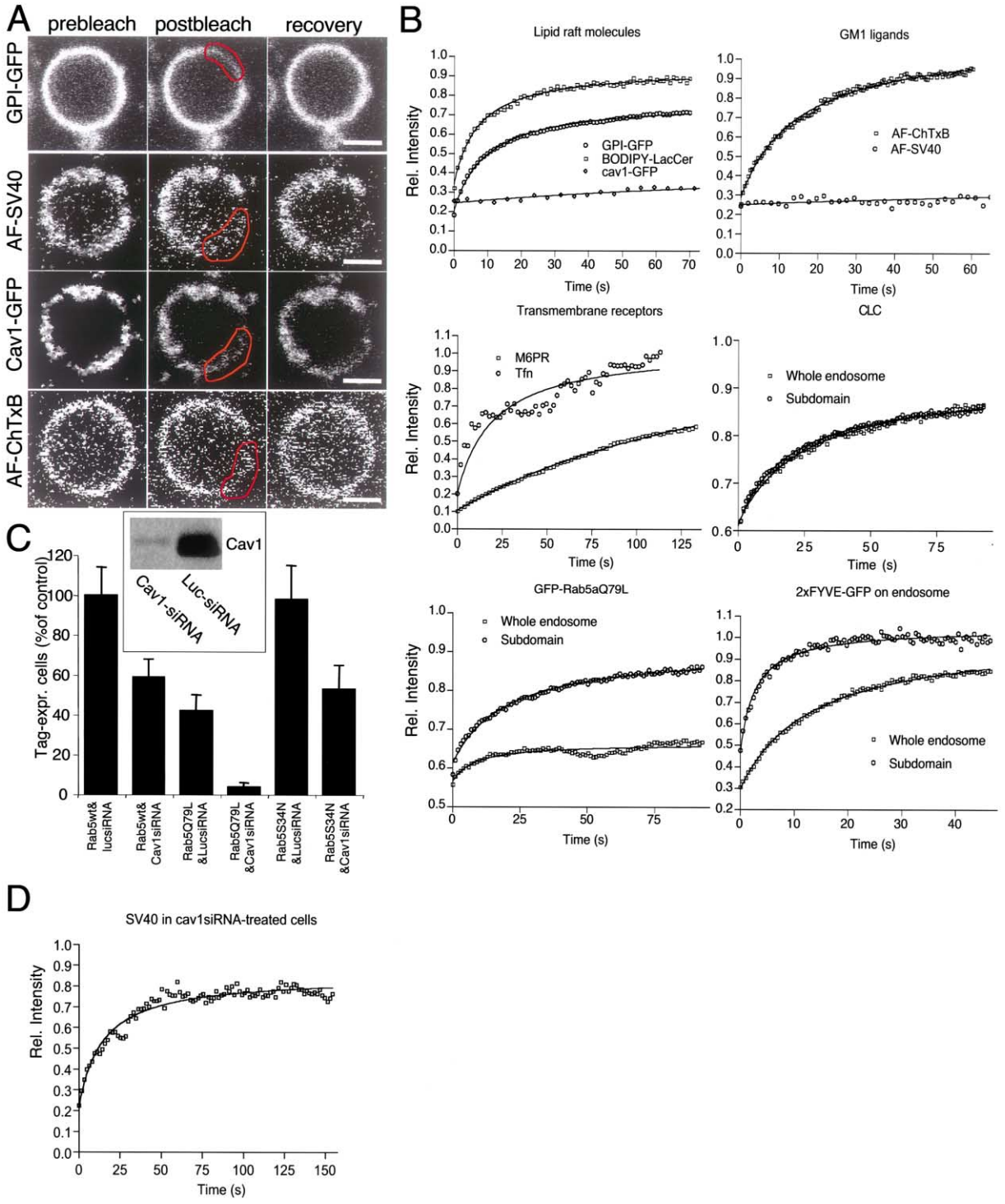

Figure 4. Caveolar Domains in Endosomes Serve as Stable Scaffolds

(A) Depicted are examples of enlarged endosomes that incorporated GPI-GFP, Cav1-GFP, AF-SV40, or AF-ChTxB imaged before and after bleaching and after recovery. Red lines indicate the region bleached. Scale bars, 1 μm.

(B) Cells transfected with Rab5Q79L were incubated with AF-ChTxB, Tfn, BODIPY-LacCer, or SV40 or cotransfected with GFP-M6PR, GFP-CLC, GFP-Rab5aQ79L, 2xFYVE-GFP, GPI-GFP, or Cav1-GFP and used for FRAP analysis. After quantification of the intensity of the bleached area as exemplified in (A) and correction for overall bleaching during imaging, recovery curves were generated. The solid lines represent curves fitted by nonlinear regression to a 2D diffusion model.

(C) SV40 infection in cells treated with a control siRNA (against luciferase) or Cav1-siRNA. Cav1 depletion (shown by Western blot) moderately (40%) reduces SV40 infection. Expression of Rab5Q79L in these cells results in a near complete (95%) block in infection. Expression of Rab5S34N in these cells has no additional effects on SV40 infection.

(D) A recovery curve and fit for AF-SV40 in an enlarged endosome of a cell treated with siRNA against Caveolin-1, showing that AF-SV40 is not restricted in its lateral mobility in the endosomal membrane.

Table 1. Curve-Fitting Values for I_0, I_{max}, T_{half}, and Immobile Fractions of FRAP Experiments

		R2	I0	Imax	Thalf (s)	Immobile Fraction
2XFYVE-GFP	Whole endosome	0.996	0.296 ± 0.009	1.017 ± 0.011	13.25 ± 0.800	−0.024 ± 0.016
	Subdomain	0.969	0.468 ± 0.028	1.045 ± 0.008	2.778 ± 0.377	−0.085 ± 0.020
GFP-Rab5Q79L	Whole endosome	0.798	0.565 ± 0.013	0.664 ± 0.005	8.097 ± 3.254	0.772 ± 0.012
	Subdomain	0.992	0.612 ± 0.006	0.908 ± 0.006	19.65 ± 1.675	0.238 ± 0.010
CLC-GFP	Whole endosome	0.988	0.616 ± 0.007	0.925 ± 0.009	25.65 ± 2.785	0.194 ± 0.019
	Subdomain	0.982	0.620 ± 0.011	0.925 ± 0.012	24.56 ± 3.130	0.196 ± 0.025
M6PR-GFP		0.998	0.107 ± 0.005	1.306 ± 0.075	196.5 ± 20.20	−0.343 ± 0.086
AF-Tfn		0.826	0.154 ± 0.048	1.034 ± 0.077	20.11 ± 9.245	−0.046 ± 0.093
GPI-GFP		0.997	0.205 ± 0.009	0.776 ± 0.005	9.502 ± 0.519	0.282 ± 0.004
Bodipy-LacCer		0.993	0.342 ± 0.015	0.941 ± 0.007	7.160 ± 0.585	0.089 ± 0.009
Cav1-GFP		0.908	0.245 ± 0.012	0.455 ± 0.123	124.2 ± 130.7	0.720 ± 0.151
AF-SV40		0.678	0.252 ± 0.012	0.494 ± 0.242	329.0 ± 506.6	0.671 ± 0.313
AF-ChTxB		0.994	0.289 ± 0.012	1.114 ± 0.013	15.17 ± 1.025	−0.160 ± 0.022
AF-SV40 (Cav1-siRNA)		0.940	0.222 ± 0.041	0.848 ± 0.017	14.66 ± 2.955	0.195 ± 0.012
AF-ChTxB (neutral pH)		0.577	0.244 ± 0.024	0.362 ± 0.016	24.21 ± 17.88	0.844 ± 0.006
AF-ChTxB (neutral pH and Cav1-siRNA)		0.978	0.380 ± 0.020	1.005 ± 0.016	13.23 ± 1.745	−0.009 ± 0.026

Curves from Figure 5 were fitted to a 2D diffusion model (see Experimental Procedures).
R^2 indicates goodness of fit and should ideally be 1. Bad fits are often caused by uncertainties about I_{max}, which is seen when molecules are immobile. The fast half-time (24 s) for AF-ChTxB at neutral pH reflects that of just a few mobile molecules not captured by caveolar domains, since the majority is captured and immobile (84%). Note that whole endosome curves of 2XFYVE-GFP, GFP-Rab5Q79L, and CLC-GFP do not reflect membrane diffusion but exchange of membrane bound molecules with cytosolic molecules. Since Rab5Q79L is fairly immobile in this curve, the curve obtained from subdomain bleaching can be regarded as reflecting diffusion within the membrane only. For 2XFYVE-GFP, the fast half-time in the subdomain-bleached curve compared to the whole endosome-bleached curve indicates fast diffusion of this probe on the membrane. For CLC-GFP, the half-time and immobile fractions in both the subdomain-bleached curve and whole endosome-bleached curve are similar. Thus, subdomain recovery consists only of exchange, indicating that CLC-GFP is immobile on the membrane. Note that both Cav1-GFP and AF-SV40 have very high half-times and show a very large immobile fraction, indicating that they are immobile.

pH inside endosomes. After accumulation in enlarged endosomes in the presence of NH_4Cl, the ChTxB did indeed localize to caveolar domains (Figure 5A). Furthermore, ChTxB was now restricted in its mobility (Figure 5B), while the recovery rates of GPI-GFP and BODIPY-LacCer upon bleaching were unaffected (data not shown). Similar results were obtained in other cells expressing only endogenous Caveolin-1 (data not shown). Apparently, at neutral pH, ChTx was not released from caveolar vesicles after fusion with endosomes or was actively sequestered in stable caveolar domains in endosomes.

In addition, we found that, in HeLa cells expressing Cav1-GFP, ChTxB accumulation in the Golgi complex was reduced in the presence of NH_4Cl (Figure 5C), while this was not perturbed in HeLa cells treated with siRNA against Caveolin-1. As expected, ChTxB was mobile on the enlarged endosomal membrane in these cells, even when treated with NH_4Cl (Figure 5B). These results suggest that caveolae-internalized ChTxB is only transported to the Golgi complex when it is released from caveolar domains, which is mediated by low pH in endosomes. Importantly, they provide an explanation for why ChTxB is immobile at early time points of internalization (Bacia et al., 2002), being present in organelles with caveolar domains and neutral pH, both on the cell surface and in caveosomes (Pelkmans et al., 2001). Furthermore, ChTxB internalized by caveolae-independent mechanisms could potentially become trapped in caveolar domains inside the cell if the route intersects with caveosomes. Finally, our data clarify the necessity for Rab5-mediated transport of ChTxB to endosomes to allow subsequent sorting to the Golgi complex.

Discussion

We have provided evidence that caveosomes and early endosomes communicate via a pathway regulated by Rab5. On the endosomal membrane, caveolar vesicles form stabilized subdomains capable of entrapping multivalent GM1 bound cargo. In endosomes, ChTxB is induced to diffuse out of these subdomains into the surrounding membrane by low pH, while SV40 remains trapped. As a result, the caveolar ligands are sorted into different endocytic compartments. Based on these observations, we propose that caveolar domains serve as specialized transport and sorting devices in intracellular membrane traffic (Figure 6). Their membrane is composed of lipids enriched in raft fractions, stabilized by a structural Caveolin-1 scaffold, and, unlike lipid rafts, they form distinct, structurally stable microdomains in any membrane of the endocytic pathway through which they traffic.

After internalization, caveolar vesicles can move in the cytosol and fuse with caveosomes. When recruited by specific small GTPases, they can also dock on target organelles such as early endosomes. After fusing with these membranes, caveolae are not disassembled but preserve their compartmentalization, retaining a unique lipid and protein composition. Preliminary evidence shows that, in cells expressing constitutively active ARF1, intracellular caveolar domains are targeted to ARF1Q71L-containing membranes, where they also form stable domains (L.P., unpublished data). We thus propose that the caveolar membrane system connects with endocytic and exocytic organelles at several levels by shuttling caveolar vesicles that maintain their stability in time and space. Because the stabilizing scaffold of

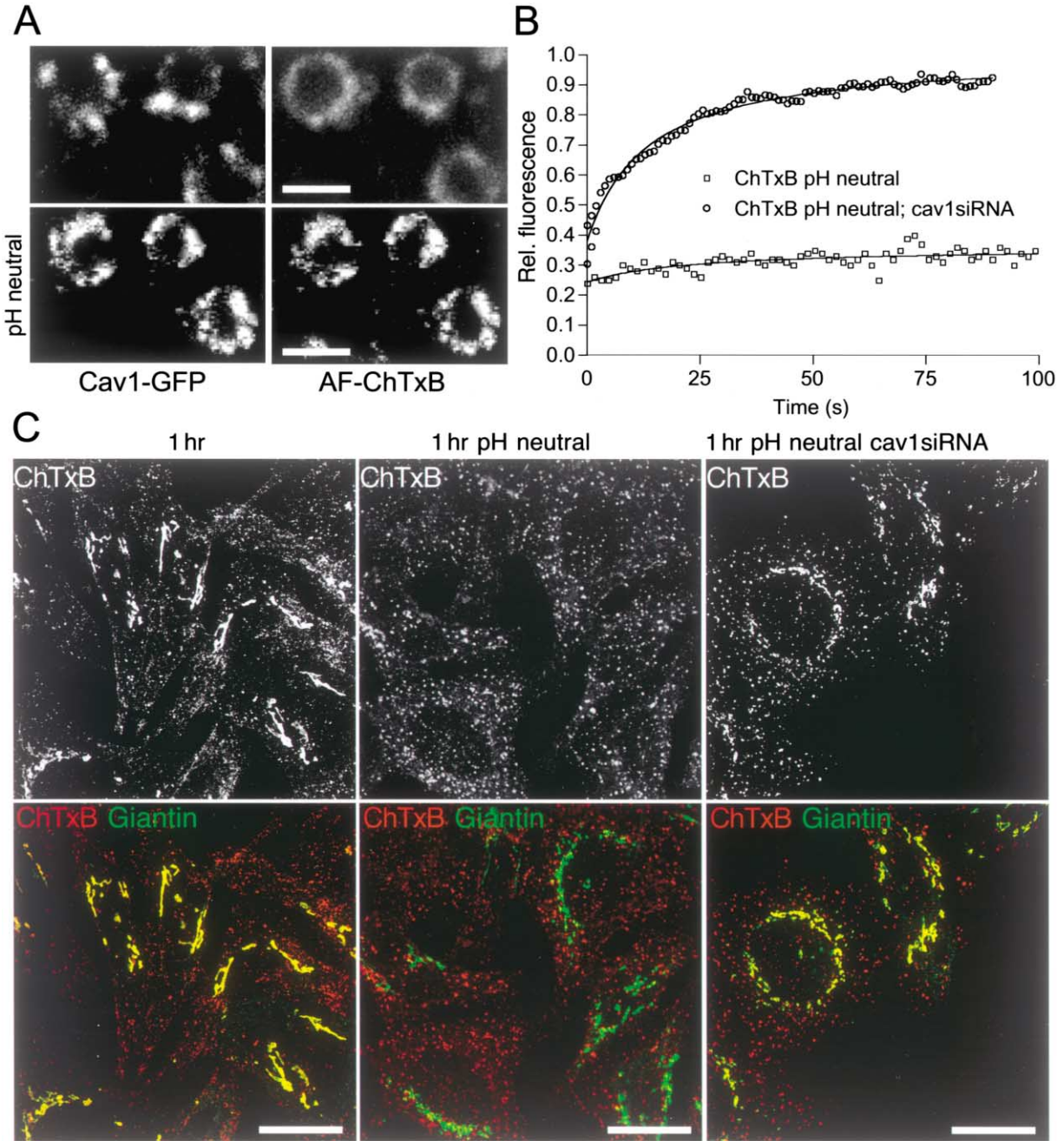

Figure 5. Low pH Triggers Release of Cholera Toxin from Caveolar Domains

(A) HeLa cells stably expressing Cav1-GFP were transfected with Rab5aQ79L and incubated with 100 pg AF-ChTxB either untreated or treated with NH_4Cl to neutralize the pH inside endosomes. Confocal images show that, while, in untreated cells, ChTxB quickly spreads evenly across the endosomal membrane, in cells treated with NH_4Cl, AF-ChTxB remains present in a patches on enlarged endosomes that colocalize with Cav1-GFP. Scale bars, 2 μm.

(B) Recovery curves of ChTxB bleached in enlarged endosomes of cells treated with NH_4Cl show that, at neutral pH, ChTxB is not released from caveolar domains. Depletion of Caveolin-1 by siRNA allows diffusion at neutral pH.

(C) In control cells, ChTxB has reached the Golgi complex after 1 hr, while, in cells treated with NH_4Cl (pH neutral), ChTxB remains trapped in endocytic structures. When cells were depleted of Caveolin-1, low pH was not necessary for ChTxB transport to the Golgi complex. Scale bars, 20 μm.

a caveolar domain is composed of oligomeric integral membrane proteins that do not dissociate, it follows along as the vesicle undergoes intracellular transport, cargo loading and unloading, and membrane fission and fusion. In so doing, its role is to define and ensure domain identity and, unlike clathrin and COP coats, not transiently but permanently. Importantly, this feature is distinct from lipid rafts, which move about the mem-

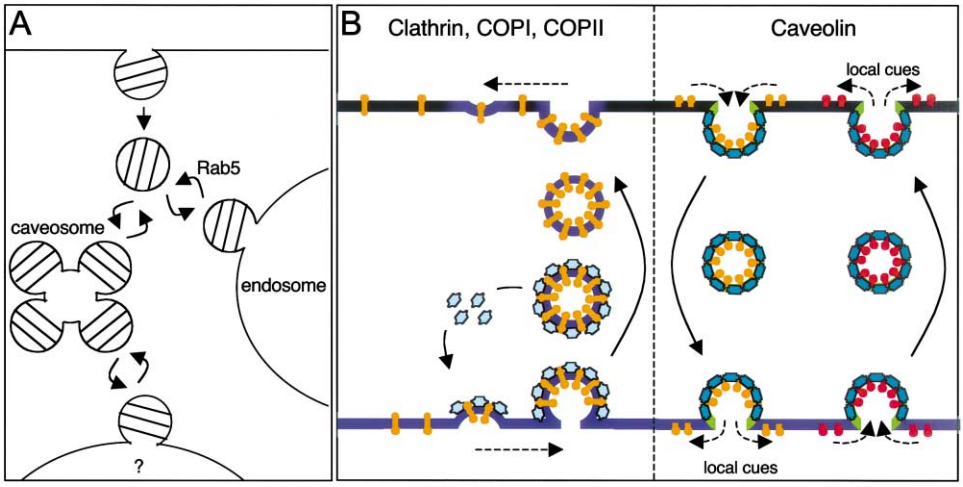

Figure 6. Working Model on Sorting by Stable Caveolar Domains

(A) Internalized caveolar vesicles are transiently targeted to early endosomes by Rab5 or interact with caveosomes. Targeting to other compartments (indicated by a question mark) likely involves transient interactions under the control of different GTPases.

(B) Contrary to cargo sorting and vesicle formation by Clathrin, COPI, and COPII coats, caveolar vesicles contain permanently stabilized membrane-integrated coats that do not undergo cyclic association and dissociation. Efficient sorting is achieved by releasing cargo in response to local cues received in a particular compartment, such as low pH in endosomes. Ligands not destined for that compartment stay trapped until arrived in a compartment that provides the right trigger for release. Cargo sequestration may also be controlled by local cues. Because caveolar vesicles retain their identity and only transiently interact, they are retrieved as such from the target membranes and can be utilized again. One advantage of such a system is that whole membrane domains including the lipids are prevented from dilution into target compartments unless triggered. This is different from vesicles formed by classical membrane coats that disassemble after vesicle formation, leading to a loss of membrane identity upon fusion with target membranes.

brane continuously and exchange lipids and proteins with surrounding nonraft membranes.

Caveolar vesicles can regulate the release of certain cargo, as exemplified by SV40 and ChTxB in endosomes. Release and uptake of caveolar cargo depends on how the cargo molecules interact with Caveolin-1, with other caveolar proteins, and with the lipids and, as revealed in this study, on how cargo is influenced by compartment-specific "cues" such as changes in pH. This mechanism allows repeated use of the domain as a transport container and still ensures high specificity of sorting. Given the enrichment of lipid rafts in caveolae, the mechanism would seem ideally suited to sort molecules that do not span the lipid bilayer, such as lipids and lipid-associated molecules, a feature not provided by classical coats and transport vesicles.

Our results provide several lines of evidence in favor of such a model. First, we showed that caveolar domains are structures in the cell that occur not only in the plasma membrane and in caveosomes but also as membrane specializations in early endosomes and possibly other compartments. This is consistent with reports using either immunolabeling of endogenous Caveolin-1 or biochemical characterization of purified endosomes (Dupree et al., 1993; Gagescu et al., 2000; Parton et al., 1994; Peters et al., 2003). In electron microscopy images, caveolar domains are often part of a larger intracellular organelle in which they share a common membrane and a common lumenal space (Pelkmans et al., 2001; Peters et al., 2003). Such domains differ from others in that they accumulate selected proteins, special lipids, and lipid bound, multivalent ligands such as SV40 and ChTx, while they exclude other endosomal regulating components such as EEA1 and PI(3)P and numerous nonraft components present in the plasma membrane.

Second, ChTxB dissociation from caveolar domains was induced by the low endosomal pH. Acidic pH is known to induce a conformational change in the ChTxB pentamer that alters the spacing of the bound GM1 molecules (McCann et al., 1997). The change in the structure of the toxin-receptor complexes may be sufficient to allow them to diffuse from the caveolar domains. SV40 particles did not respond to the low pH in endosomes. They remained associated with the immobile caveolar domains. Only when Caveolin-1 was downregulated by siRNA were the viruses free to diffuse in the endosomal membrane. That this did not lead to infection confirmed that the normal pathway over caveosomes and the ER is needed for productive entry. From our previous studies, we know that SV40 particles are at some point released from caveolar domains and move to the ER in Caveolin-1-free tubules and vesicles (Pelkmans et al., 2001). It remains to be shown which GTPase regulates the targeting of caveolar domains to these membranes and by what cue the virus is released.

In cells expressing constitutively active Rab5, most intracellular caveolar domains were associated with early endosomes. The arrival of Cav1-GFP-labeled caveolar vesicles could be seen in live cell imaging of the enlarged endosomes. Caveolae-internalized SV40 was now directed to endosomes, confirming that Rab5 strongly promotes caveolar traffic to early endosomes. Although Rab5-dependent transport via endosomes was not obligatory for SV40 infection, it was a necessary step for ChTxB to dissociate from caveolar domains and accumulate in the Golgi complex. The dependence on

Rab5 excluded the possibility that caveolar vesicles would be directly targeted to the Golgi complex where the mildly acidic pH of the trans-Golgi network may potentially release ChTxB from caveolar domains. Importantly, when we allowed more toxin to enter cells (L.P., unpublished data), the dependence on Rab5 and low pH to reach the Golgi complex decreased, consistent with observations that the toxin can take pathways that are caveolae independent and therefore do not require toxin release from caveolin-1-stabilized domains in endosomes.

FRAP analysis illustrated the remarkable stability of caveolar domains, underscored the complexity of the membranes in the endocytic pathway, and confirmed the presence of numerous different membrane subdomains (Gruenberg, 2001; Zerial and McBride, 2001). Although precise kinetic measurements require further technical improvements, we were clearly able to distinguish classes of molecules in the enlarged endosomes with different mobility. Clathrin-containing domains were immobile, while mannose-6-phosphate receptor-containing domains displayed intermediate mobility and Tfn-containing domains unrestricted mobility. The limited mobility of Rab5Q79L in all likelihood reflected the engagement of this GTPase in oligomeric complexes of effectors on the endosomal membrane (McBride et al., 1999). The molecules with the highest mobility were BODIPY-LacCer, a lipid probe (Kaiser and London, 1998), and GPI-anchored GFP, which partitions into lipid rafts via its GPI-anchor (Keller et al., 2001), illustrating that the stability of caveolar domains is not a general property of lipid rafts. 2XFYVE-GFP, a probe that binds to the early endosomal lipid PI(3)P on the cytosolic leaflet, also showed unrestricted mobility.

Finally, the mechanism proposed may have other functions in the cell besides the sorting of glycosphingolipid bound ligands. For instance, it may be used by GPI-anchored prion protein en route to late endosomes (Peters et al., 2003) or to control the signaling of transforming growth factor β receptors (TGFβ-R). These receptors are internalized into early endosomes, where they activate signaling, but can be sequestered by caveolin-1 into caveolar membranes, where they cannot activate signaling (Di Guglielmo et al., 2003; Razani et al., 2001). Intriguingly, expression of Rab5S34N was found to strongly increase signaling by TGFβ-R (Panopoulou et al., 2002). In line with our observations, this may be due to a reduced interaction of caveolar domains with early endosomes and thus a reduced inactivation of TGFβ-R signaling. Such roles for caveolar domains in the endocytic pathway will have to be addressed in future studies.

Experimental Procedures

Antibodies, cDNAs, and Reagents

Antibodies against EEA1 and large T antigen are described elsewhere (Pelkmans et al., 2001). Fluorophores and fluorescently labeled ChTxB, LacCer, and Tfn were from Molecular Probes (Leiden, The Netherlands). SV40 was purified and labeled with Alexa Fluor as previously described (Pelkmans et al., 2001). Plasmids encoding Caveolin-1, Rab4, Rab5, Rab6, Rab7, Rab9, Rab11, M6PR, CLC, and GPI-anchor have been described (Barbero et al., 2002; Gaidarov et al., 1999; Keller et al., 2001; Lebrand et al., 2002; Pelkmans et al., 2001; Presley et al., 2002; Sonnichsen et al., 2000; Waguri et al., 2003; White et al., 1999).

Transfection of cDNA and siRNA

Cells were transiently transfected with FuGENE and used 16 hr after transfection. Stably transfected HeLa cell lines were maintained in medium containing 500 μg/ml G418. siRNA against human Caveolin-1 was transfected into HeLa cells with Oligofectamine. After transfection (3–4 days), cells were used for experiments.

Deconvolution, 3D Reconstruction, and Overlap Quantification

Z stacks were processed with a classical maximum likelihood estimation (CLME) deconvolution algorithm (McNally et al., 1999) and subsequently used to make surface-rendered 3D reconstructions. For 2D representations, maximum projections were made of the deconvolved stacks. Overlap quantification was done on each image of a deconvolved Z stack using ImageJ software as described previously (Pelkmans et al., 2001).

Subdomain Bleaching on Endosomes and Computational Analysis of Mobility

First, a region of interest was drawn around the area to bleach. Using maximum laser power at the required wavelength and an empirically determined number of iterations, the signal in the region of interest was bleached to levels 20%–60% of the original intensity. Bleaching time was usually less then 5 s. After bleaching, 100 images with 1 s intervals were usually taken to monitor recovery. When necessary, endosomes were manually tracked and the region of interest redrawn in order to correct for endosome movement during the recovery period. Obtained data were corrected for bleaching during imaging (Pelkmans et al., 2001) and fitted to a function for lateral diffusion, which assumes that recovery involves a single diffusion coefficient and that there is no membrane flow (Yguerabide et al., 1982):

$$I(t) = \frac{1_0 + (1_{\max} \cdot t)/T_{\text{half}}}{1 + t/T_{half}} \quad (1)$$

Using the experimentally obtained values for $I(t)$, the values for I_0, I_{max}, and T_{half} were calculated with nonlinear regression to Equation 1 without any constraints using Prism4 (Graphpad, San Diego, CA).

Acknowledgments

We thank Jean Gruenberg, Alice Dautry-Varsat, Suzanne Pfeffer, John Colicelli, and Jim Keen for plasmids; and Doris Meder, Carsten Schnatwinkel, and Kai Simons for critical reading of the manuscript. This work was supported by the SNF, EU, and ETHZ (to A.H.) and by the Human Frontiers Science Program and Max Planck Society (to M.Z.). L.P. is a recipient of a long-term EMBO fellowship.

Received: February 3, 2004
Revised: August 16, 2004
Accepted: August 21, 2004
Published: September 16, 2004

References

Anderson, R.G.W. (1998). The caveolae membrane system. Annu. Rev. Biochem. *67*, 199–225.

Anderson, H.A., Chen, Y., and Norkin, L.C. (1996). Bound simian virus 40 translocates to caveolin-enriched membrane domains, and its entry is inhibited by drugs that selectively disrupt caveolae. Mol. Biol. Cell *7*, 1825–1834.

Bacia, K., Majoul, I.V., and Schwille, P. (2002). Probing the endocytic pathway in live cells using dual-color fluorescence cross-correlation analysis. Biophys. J. *83*, 1184–1193.

Barbero, P., Bittova, L., and Pfeffer, S.R. (2002). Visualization of Rab9-mediated vesicle transport from endosomes to the trans-Golgi in living cells. J. Cell Biol. *156*, 511–518.

Benmerah, A., Bayrou, M., Cerf-Bensussan, N., and Dautry-Varsat,

A. (1999). Inhibition of clathrin-coated pit assembly by an Eps15 mutant. J. Cell Sci. *112*, 1303–1311.

Campbell, R.E., Tour, O., Palmer, A.E., Steinbach, P.A., Baird, G.S., Zacharias, D.A., and Tsien, R.Y. (2002). A monomeric red fluorescent protein. Proc. Natl. Acad. Sci. USA *99*, 7877–7882.

Conner, S.D., and Schmid, S.L. (2003). Regulated portals of entry into the cell. Nature *422*, 37–44.

Di Guglielmo, G.M., Le Roy, C., Goodfellow, A.F., and Wrana, J.L. (2003). Distinct endocytic pathways regulate TGF-beta receptor signalling and turnover. Nat. Cell Biol. *5*, 410–421.

Drab, M., Verkade, P., Elger, M., Kasper, M., Lohn, M., Lauterbach, B., Menne, J., Lindschau, C., Mende, F., Luft, F.C., et al. (2001). Loss of caveolae, vascular dysfunction, and pulmonary defects in caveolin-1 gene-disrupted mice. Science *293*, 2449–2452.

Dupree, P., Parton, R.G., Raposo, G., Kurzchalia, T.V., and Simons, K. (1993). Caveolae and sorting in the trans-Golgi network of epithelial cells. EMBO J. *12*, 1597–1605.

Fernandez, I., Ying, Y., Albanesi, J., and Anderson, R.G. (2002). Mechanism of caveolin filament assembly. Proc. Natl. Acad. Sci. USA *99*, 11193–11198.

Fra, A.M., Williamson, E., Simons, K., and Parton, R.G. (1995). De novo formation of caveolae in lymphocytes by expression of VIP21-caveolin. Proc. Natl. Acad. Sci. USA *92*, 8655–8659.

Gagescu, R., Demaurex, N., Parton, R.G., Hunziker, W., Huber, L.A., and Gruenberg, J. (2000). The recycling endosome of Madin-Darby canine kidney cells is a mildly acidic compartment rich in raft components. Mol. Biol. Cell *11*, 2775–2791.

Gaidarov, I., Santini, F., Warren, R.A., and Keen, J.H. (1999). Spatial control of coated-pit dynamics in living cells. Nat. Cell Biol. *1*, 1–7.

Gillooly, D.J., Morrow, I.C., Lindsay, M., Gould, R., Bryant, N.J., Gaullier, J.M., Parton, R.G., and Stenmark, H. (2000). Localization of phosphatidylinositol 3-phosphate in yeast and mammalian cells. EMBO J. *19*, 4577–4588.

Gruenberg, J. (2001). The endocytic pathway: a mosaic of domains. Nat. Rev. Mol. Cell Biol. *2*, 721–730.

Heyningen, S.V. (1974). Cholera toxin: interaction of subunits with ganglioside GM1. Science *183*, 656–657.

Janicot, M., Fouque, F., and Desbuquois, B. (1991). Activation of rat liver adenylate cyclase by cholera toxin requires toxin internalization and processing in endosomes. J. Biol. Chem. *266*, 12858–12865.

Kaiser, R.D., and London, E. (1998). Determination of the depth of BODIPY probes in model membranes by parallax analysis of fluorescence quenching. Biochim. Biophys. Acta *1375*, 13–22.

Kartenbeck, J., Stukenbrok, H., and Helenius, A. (1989). Endocytosis of simian virus 40 into the endoplasmic reticulum. J. Cell Biol. *109*, 2721–2729.

Keller, P., Toomre, D., Diaz, E., White, J., and Simons, K. (2001). Multicolour imaging of post-Golgi sorting and trafficking in live cells. Nat. Cell Biol. *3*, 140–149.

Lanzetti, L., Rybin, V., Malabarba, M.G., Christoforidis, S., Scita, G., Zerial, M., and Di Fiore, P.P. (2000). The Eps8 protein coordinates EGF receptor signalling through Rac and trafficking through Rab5. Nature *408*, 374–377.

Lebrand, C., Corti, M., Goodson, H., Cosson, P., Cavalli, V., Mayran, N., Faure, J., and Gruenberg, J. (2002). Late endosome motility depends on lipids via the small GTPase Rab7. EMBO J. *21*, 1289–1300.

McBride, H.M., Rybin, V., Murphy, C., Giner, A., Teasdale, R., and Zerial, M. (1999). Oligomeric complexes link Rab5 effectors with NSF and drive membrane fusion via interactions between EEA1 and syntaxin 13. Cell *98*, 377–386.

McCann, J.A., Mertz, J.A., Czworkowski, J., and Picking, W.D. (1997). Conformational changes in cholera toxin B subunit-ganglioside GM1 complexes are elicited by environmental pH and evoke changes in membrane structure. Biochemistry *36*, 9169–9178.

McNally, J.G., Karpova, T., Cooper, J., and Conchello, J.A. (1999). Three-dimensional imaging by deconvolution microscopy. Methods *19*, 373–385.

Mellman, I. (1996). Endocytosis and molecular sorting. Annu. Rev. Cell Dev. Biol. *12*, 575–625.

Monier, S., Parton, R.G., Vogel, F., Behlke, J., Henske, A., and Kurzchalia, T.V. (1995). VIP21-caveolin, a membrane protein constituent of the caveolar coat, oligomerizes in vivo and in vitro. Mol. Biol. Cell *6*, 911–927.

Murata, M., Peranen, J., Schreiner, R., Wieland, F., Kurzchalia, T.V., and Simons, K. (1995). VIP21/caveolin is a cholesterol-binding protein. Proc. Natl. Acad. Sci. USA *92*, 10339–10343.

Nichols, B.J. (2002). A distinct class of endosome mediates clathrin-independent endocytosis to the Golgi complex. Nat. Cell Biol. *4*, 374–378.

Orlandi, P.A., and Fishman, P.H. (1998). Filipin-dependent inhibition of cholera toxin: evidence for toxin internalization and activation through caveolae-like domains. J. Cell Biol. *141*, 905–915.

Panopoulou, E., Gillooly, D.J., Wrana, J.L., Zerial, M., Stenmark, H., Murphy, C., and Fotsis, T. (2002). Early endosomal regulation of Smad-dependent signaling in endothelial cells. J. Biol. Chem. *277*, 18046–18052.

Parton, R.G., and Richards, A.A. (2003). Lipid rafts and caveolae as portals for endocytosis: new insights and common mechanisms. Traffic *4*, 724–738.

Parton, R.G., Joggerst, B., and Simons, K. (1994). Regulated internalization of caveolae. J. Cell Biol. *127*, 1199–1215.

Pelkmans, L., Kartenbeck, J., and Helenius, A. (2001). Caveolar endocytosis of simian virus 40 reveals a new two-step vesicular-transport pathway to the ER. Nat. Cell Biol. *3*, 473–483.

Pelkmans, L., Puntener, D., and Helenius, A. (2002). Local actin polymerization and dynamin recruitment in SV40-induced internalization of caveolae. Science *296*, 535–539.

Peters, P.J., Mironov, A., Jr., Peretz, D., van Donselaar, E., Leclerc, E., Erpel, S., DeArmond, S.J., Burton, D.R., Williamson, R.A., Vey, M., and Prusiner, S.B. (2003). Trafficking of prion proteins through a caveolae-mediated endosomal pathway. J. Cell Biol. *162*, 703–717.

Pfeffer, S. (2003). Membrane domains in the secretory and endocytic pathways. Cell *112*, 507–517.

Presley, J.F., Ward, T.H., Pfeifer, A.C., Siggia, E.D., Phair, R.D., and Lippincott-Schwartz, J. (2002). Dissection of COPI and Arf1 dynamics in vivo and role in Golgi membrane transport. Nature *417*, 187–193.

Puri, V., Watanabe, R., Singh, R.D., Dominguez, M., Brown, J.C., Wheatley, C.L., Marks, D.L., and Pagano, R.E. (2001). Clathrin-dependent and -independent internalization of plasma membrane sphingolipids initiates two Golgi targeting pathways. J. Cell Biol. *154*, 535–547.

Razani, B., Zhang, X.L., Bitzer, M., von Gersdorff, G., Bottinger, E.P., and Lisanti, M.P. (2001). Caveolin-1 regulates transforming growth factor (TGF)-beta/SMAD signaling through an interaction with the TGF-beta type I receptor. J. Biol. Chem. *276*, 6727–6738.

Richards, A.A., Stang, E., Pepperkok, R., and Parton, R.G. (2002). Inhibitors of COP-mediated transport and cholera toxin action inhibit simian virus 40 infection. Mol. Biol. Cell *13*, 1750–1764.

Rothberg, K.G., Heuser, J.E., Donzell, W.C., Ying, Y.S., Glenney, J.R., and Anderson, R.G. (1992). Caveolin, a protein component of caveolae membrane coats. Cell *68*, 673–682.

Sandvig, K., and van Deurs, B. (2002). Transport of protein toxins into cells: pathways used by ricin, cholera toxin and Shiga toxin. FEBS Lett. *529*, 49–53.

Sonnichsen, B., De Renzis, S., Nielsen, E., Rietdorf, J., and Zerial, M. (2000). Distinct membrane domains on endosomes in the recycling pathway visualized by multicolor imaging of Rab4, Rab5, and Rab11. J. Cell Biol. *149*, 901–913.

Stang, E., Kartenbeck, J., and Parton, R.G. (1997). Major histocompatibility complex class I molecules mediate association of SV40 with caveolae. Mol. Biol. Cell *8*, 47–57.

Stenmark, H., Parton, R.G., Steele-Mortimer, O., Lutcke, A., Gruenberg, J., and Zerial, M. (1994). Inhibition of rab5 GTPase activity stimulates membrane fusion in endocytosis. EMBO J. *13*, 1287–1296.

Tall, G.G., Barbieri, M.A., Stahl, P.D., and Horazdovsky, B.F. (2001). Ras-activated endocytosis is mediated by the Rab5 guanine nucleotide exchange activity of RIN1. Dev. Cell *1*, 73–82.

Thomsen, P., Roepstorff, K., Stahlhut, M., and van Deurs, B. (2002). Caveolae are highly immobile plasma membrane microdomains, which are not involved in constitutive endocytic trafficking. Mol. Biol. Cell *13*, 238–250.

Tran, D., Carpentier, J.L., Sawano, F., Gorden, P., and Orci, L. (1987). Ligands internalized through coated or noncoated invaginations follow a common intracellular pathway. Proc. Natl. Acad. Sci. USA *84*, 7957–7961.

Tsai, B., Gilbert, J.M., Stehle, T., Lencer, W., Benjamin, T.L., and Rapoport, T.A. (2003). Gangliosides are receptors for murine polyoma virus and SV40. EMBO J. *22*, 4346–4355.

Upcroft, P. (1987). Simian virus 40 infection is not mediated by lysosomal activation. J. Gen. Virol. *678*, 2477–2480.

Waguri, S., Dewitte, F., Le Borgne, R., Rouille, Y., Uchiyama, Y., Dubremetz, J.F., and Hoflack, B. (2003). Visualization of TGN to endosome trafficking through fluorescently labeled MPR and AP-1 in living cells. Mol. Biol. Cell *14*, 142–155.

White, J., Johannes, L., Mallard, F., Girod, A., Grill, S., Reinsch, S., Keller, P., Tzschaschel, B., Echard, A., Goud, B., and Stelzer, E.H. (1999). Rab6 coordinates a novel Golgi to ER retrograde transport pathway in live cells. J. Cell Biol. *147*, 743–760.

Yguerabide, J., Schmidt, J.A., and Yguerabide, E.E. (1982). Lateral mobility in membranes as detected by fluorescence recovery after photobleaching. Biophys. J. *40*, 69–75.

Zerial, M., and McBride, H. (2001). Rab proteins as membrane organizers. Nat. Rev. Mol. Cell Biol. *2*, 107–117.